DOI 10.1007/s10946-014-9458-8
Journal of Russian Laser Research, Volume 35, Number 6, November, 2014

DISTRIBUTED-FEEDBACK SOLID-STATE POLYMERIC-DYE LASERS BASED ON EXCITATION-ENERGY TRANSFER

G. V. Vijayaraghavan and M. Basheer Ahamed*

Department of Physics
B. S. Abdur Rahman University
Chennai, India

*Corresponding author e-mail: basheerahamed@bsauniv.ac.in

Abstract

Using Q-switched Nd:YAG laser excitation, we investigate both theoretically and experimentally the energy transfer between dyes Pyronin-Y (PY) and cresyl violet (CV) incorporated in a methyl methacrylate (MMA) matrix. From the absorption and fluorescence spectral data of PY and CV dyes, we calculate the absorption and emission cross-section of donor and acceptor dye molecules, the critical transfer radius R_0, the critical concentration C_0, the half-quenching concentration $C_{1/2}$, and the Foster-type transfer rate k_f. We study the influence of donor–acceptor concentration and pump power on the energy transfer and its mechanism. Both energy transfer phenomenon and the self-absorption mechanism play a role in laser tunability. We achieve a tuning of the output wavelength (between 580 and 670 nm) by varying the periodic gain modulation generated by a Q-switched Nd:YAG laser.

Keywords: energy-transfer dye laser, solid-state dye laser, wavelength tuning, MMA, polymerization.

1. Introduction

The first solid-state dye lasers, using polymer matrices, were reported around 1960 by Soffer and McFarland [1] and Peterson and Snavely [2]. Solid-state dye lasers are nontoxic and maintenance-free, compared with liquid dye lasers [3–5]. Hence, they have been preferably used in solar cells, atmospheric and underwater sensing, isotope separation, and spectroscopy [6, 7]. Solid-state organic polymer-based lasers give emission from near UV to near IR range, similar to liquid dye-laser emission. It is well known that organic dyes have a broad energy band and can be easily embedded into the host material, such as polymers [8, 9]. Importantly, flow fluctuation and solvent evaporation are avoided in solid-state dye lasers [10].

Since the tunability of dye lasers depends mainly on the energy-transfer mechanism in the laser dye mixture, much research attention has focused on the identification and combinations of suitable dyes. Energy-transfer dye lasers based on various donor–acceptor pairs have been well demonstrated [11–13]. These have used the distributed feedback (DFB) mechanism to generate subnanosecond pulses [14]. Noticeably, DFB produces a narrow band and frequency-tunable coherent radiation. Together with the self Q-switching technique, laser pulses that are 50–100 times shorter than the pump pulse could be obtained. The feedback is strongly frequency selective, and the resonant mode for laser oscillation satisfies well the Bragg condition [15–17]. In such lasers, wavelength tunability can be achieved by changing the

Manuscript submitted by the authors in English first on October 9, 2013 and in final form on January 19, 2014.

angle between the two pump beams or by changing the refractive index of the medium, without employing any frequency-selective element in the cavity [18, 19].

Energy-transfer dye lasers based on various pumping schemes have been reported in the literature [20–22]. The energy transfer between a donor and an acceptor could be modulated via the energy migration. This modulation of energy transfer depends upon the relative strengths of interaction between the donor–acceptor (α) and donor–donor (β) molecules. The efficiency of the excitation energy transfer is proportional to the spectral overlap of the fluorescence of the donor and the absorption of the acceptor. Rhodamine 6G (Rh6G) – cresyl violet (CV) is one of the popular energy transfer systems [22, 23]. The addition of Rh6G was reported to enhance the lasing efficiency of CV [24]. Using this system, Basheer et al. have reported the pump-power dependence and effect of the acceptor concentration in a prism-type geometry [14, 25, 26].

In this work, we make an attempt to study the mechanism of energy transfer between Pyronin-Y (PY; donor) and CV (acceptor) incorporated into a solid matrix of methyl methacrylate (MMA) in a prism dye-cell arrangement. Upon optical pumping, the donor dye molecules absorb the pump energy, are excited, and release energy to be absorbed by the acceptor dye molecules. The output energy of this distributed-feedback dye laser (DFDL) was measured at the emission peaks of donor and acceptor dyes for different pump powers and acceptor concentrations, and its tunability was observed between 580 and 670 nm.

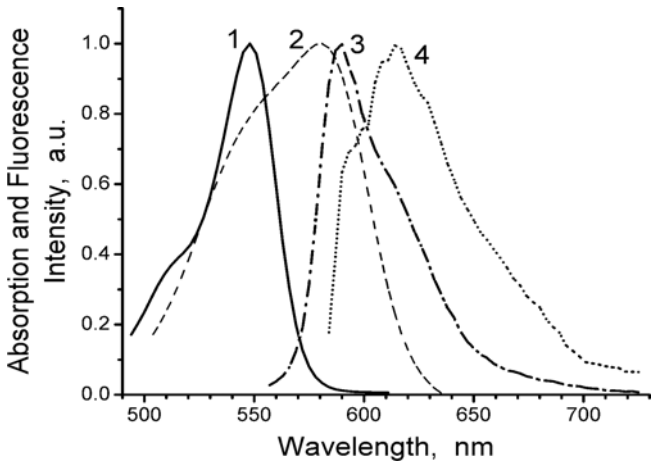

Fig. 1. Absorption and fluorescence spectra of PY and CV. Here, PY absorption (curve 1), PY fluorescence (curve 2), CV absorption (curve 3), and CV fluorescence (curve 4).

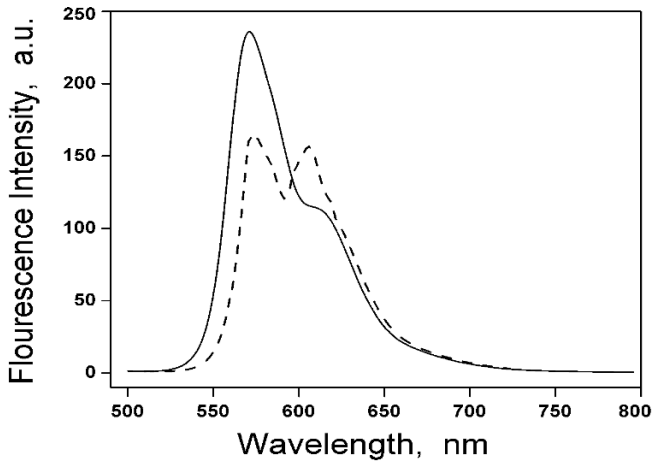

Fig. 2. Fluorescence spectra of PY-doped with MMA film in the absence (solid curve) and presence of CV (dashed curve).

2. Theoretical Studies

Applying the rate equations [25] and solving it using the fourth-order Runge–Kutta method, we study theoretically the behavior of our DFDL. From Fig. 1, the emission spectra of the donor (PY) are seen to overlap with that of the acceptor (CV). Similarly, donor–donor (DD) or acceptor–acceptor (AA) transport of excitation energy is evident from absorption and fluorescence spectra of donor and acceptor dyes, respectively. Hence, both radiative and Forster types of energy transfer have occurred between the two dyes. The fluorescence spectra (Fig. 2) of the dyes doped with MMA do not reveal

any new fluorescent peak, and hence there was no complex formation. Since the concentration of donor and acceptor molecules was less than 5.0 mM, a collisional type of energy transfer was not expected. Therefore, for the dyes considered in this work, collisional and complexing types of energy transfer were ruled out under our experimental condition. From the observed absorption and fluorescence spectra of the dyes, we calculated the spectral parameters using the rate-equation model (presented in Table 1).

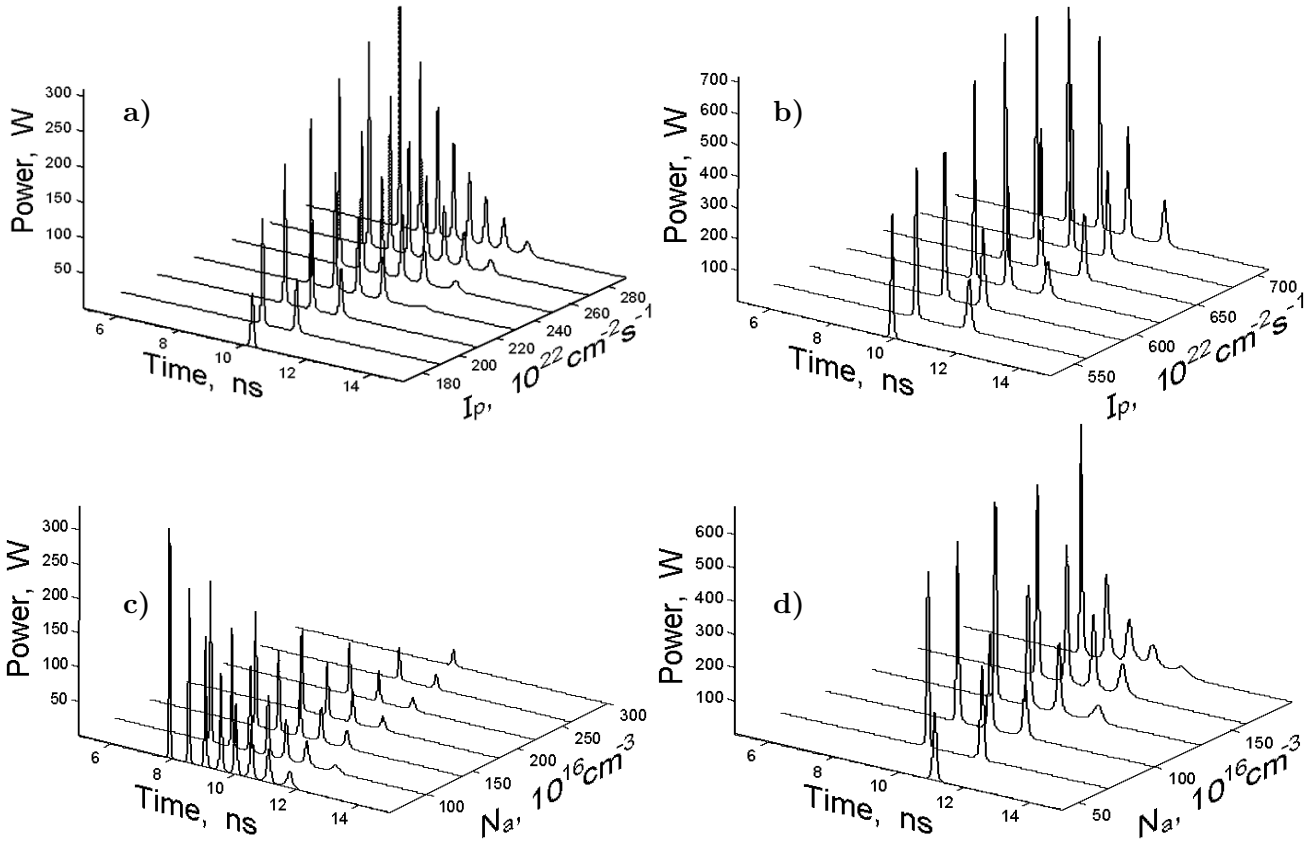

Fig. 3. Variations in the pulse width and peak output power of the donor DFDL (a) and the acceptor DFDL (b) at fixed donor ($N_{\rm d} = 1.8{\cdot}10^{18}$ cm^{-3}) and acceptor ($N_{\rm a} = 0.6{\cdot}10^{18}$ cm^{-3}) concentrations for different pump intensities. Variations in the pulse width and peak output power of the donor DFDL (c) and the acceptor DFDL (d) at fixed donor concentration ($N_{\rm d} = 1.8 \cdot 10^{18}$ cm^{-3}) and pump intensity ($I_{\rm p} = 0.6 \cdot 10^{22}$ cm$^{-2}{\cdot}$s^{-1}) for different acceptor concentrations.

3. Results

The emission of PY was in the wavelength range of 580–622 nm, with its peak at 593 nm. Similarly, the emission of CV was in the wavelength range of 583–670 nm, with its peak at 625 nm. We studied the DFDL output at donor and acceptor lasing peak wavelengths. The threshold of the first pulse and its starting time and the threshold of other pulses, expressed as a function of the pump power, are shown in Fig. 3 a and b. When a high pump power was applied, the DFDL pulse emerged sooner and with high output power, although the pulse width appeared smaller. Clearly, an increase in the pump rate had

Table 1. Spectral Parameters of Pyronin-Y and Cresyl Violet Used in the Rate-Equation Model.

Symbols	Meaning of symbol	Numerical value
τ_d	Donor lifetime	2.833 ns
τ_a	Acceptor lifetime	2.509 ns
R_0	Critical transfer radius	34.67 Å
C_0	Critical concentration	$4.97 \cdot 10^{18}$ cm^{-3}
$C_{1/2}$	Half-quenching concentration	$2.485 \cdot 10^{18}$ cm^{-3}
k_F	Forster-type transfer rate	$2.03 \cdot 10^{-10}$ cm^3/s
σ_{pd}	Absorption cross section of donor dye at a pumping wavelength of 532 nm	$2.343 \cdot 10^{-16}$ cm^2
σ_{pa}	Absorption cross section of acceptor dye at a pumping wavelength of 532 nm	$0.336 \cdot 10^{-16}$ cm^2
σ_{edl}	Emission cross section of donor dye molecules at the lasing wavelength ($\lambda_l = 593$ nm) of donor	$7.123 \cdot 10^{-16}$ cm^2
σ_{aal}	Ground-state absorption cross section of acceptor dye molecules at the lasing wavelength ($\lambda_l = 593$ nm)	$0.493 \cdot 10^{-16}$ cm^2
σ_{eal}	Emission cross section of donor dye molecules at the lasing wavelength ($\lambda_l = 593$ nm) of donor	$3.05 \cdot 10^{-16}$ cm^2
σ_{eaa}	Emission cross section of acceptor dye molecules at the lasing wavelength ($\lambda_l = 593$ nm)	$5.440 \cdot 10^{-16}$ cm^2
L	Length of the transversely excited region	0.9 cm
b	Height of the transversely excited region	0.02 cm
c	Speed of light	$3 \cdot 10^{10}$ cm $\cdot$ s^{-1}
n	Refractive index of the solvent	1.3628
n_p	Refractive index of the prism	1.52
V	Visibility of the interference pattern	0.4
S	Spectral factor contributing to spontaneous emission	10^4
Ω_d	Factor determining the fraction of the spontaneously emitted photons by excited donor and acceptor dye molecules, respectively	$1.227 \cdot 10^{-9}$
Ω_a		$0.39 \cdot 10^{-7}$

resulted in faster buildup of the population inversion. When still more pump power was applied, a second DFDL pulse emerged. The results suggest that the DFDL emission at the donor wavelength depended on the acceptor concentration. With increase in the acceptor concentration, the number of DFDL pulses at the donor wavelength decreased. Also, the output power of a single pulse decreased with increase in the pulse width and, as a result, the DFDL pulse emerged late (Fig. 3 c). In the case of DFDL emission at the acceptor wavelength, as the acceptor concentration increases, the number of DFDL pulses and the peak power were found to increase with decrease of the pulse width, as shown in Fig. 3 d.

4. Experimental

4.1. Materials

Dyes Pyronin-Y (PY, C.I. 45005, Pyronin) and cresyl violet (CV, C.I. 42555, triarylmethane) (chemical structures in Fig. 4) were purchased from Sigma Alrich, Mumbai, India. Spectroscopic-grade ethanol was used as a solvent. The absorption spectra of the dyes were recorded using a UV-VIS spectrometer (Perkin Elmer-LS25), and their fluorescence spectra measured using a fluorescence spectrometer (Perkin Elmer-LS45). Fluorescence lifetimes of the dyes were obtained using a single photon counting spectrometer. For pumping, the second harmonic of a 6 ns Nd:YAG laser (model LAB-170-10; Quanta Ray) of 10 Hz repetition rate was used.

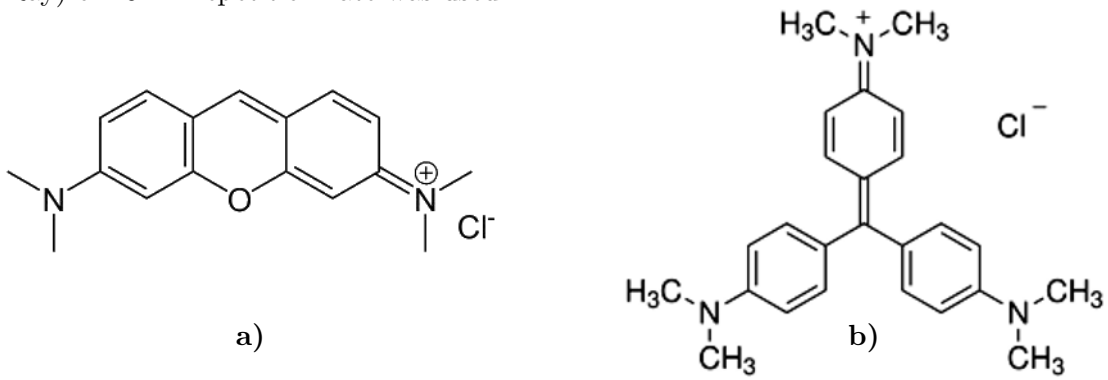

Fig. 4. Molecular formulas and chemical structures of PY and CV with molecular formula $C_{17}H_{19}N_2OCl$ and molecular weight 302.8 g·mol^{-1} (a), and molecular formula $C_{25}H_{30}N_3Cl$ and molecular weight 407.98 g·mol^{-1} (b).

4.2. Polymer Matrix Preparation

The polymer matrix was prepared by the bulk polymerization method. First, dyes in concentration as small as 10^{-3} M was taken, because a high concentration of dyes could reduce the photostability of the host material or lead to aggregation of dye molecules to form dimers. The monomer (MMA) and the ethanol were taken in the ratio of 4 : 1. A dye mixture containing a 3 mM solution of Pyronin-Y and 1 mM solution of cresyl violet was prepared. The dyes were dissolved in ethanol. To eliminate impurities from the monomer (MMA), it was mixed with aqueous sodium hydroxide, filtered, and distilled thrice. Benzyl peroxide (3 g/l) was used to initiate polymerization. Polymerization was carried out under controlled temperature conditions (70°C) using a constant temperature bath. The thickness of the dye-doped polymer film so obtained was 45.57 μm, as measured by FE-SEM.

4.3. Experimental Setup

The sides of an isosceles right-angled quartz prism (BCDE) were coated by the dye-doped polymer using the spin-coating method (Fig. 5 a). The distributed-feedback dye laser (DFDL) was obtained using the quartz prism. The prism dye-doped film set-up was used for the creation of the interference pattern on the surface of the dye cell. The pump beam (532 nm) was focused by a cylindrical quartz lens (focal length 5 cm) into a line image using a Q-switched Nd:YAG laser and made incident on the hypotenuse AB of the prism. Light transmitted by the hypotenuse of the prism was totally reflected from side AC of the

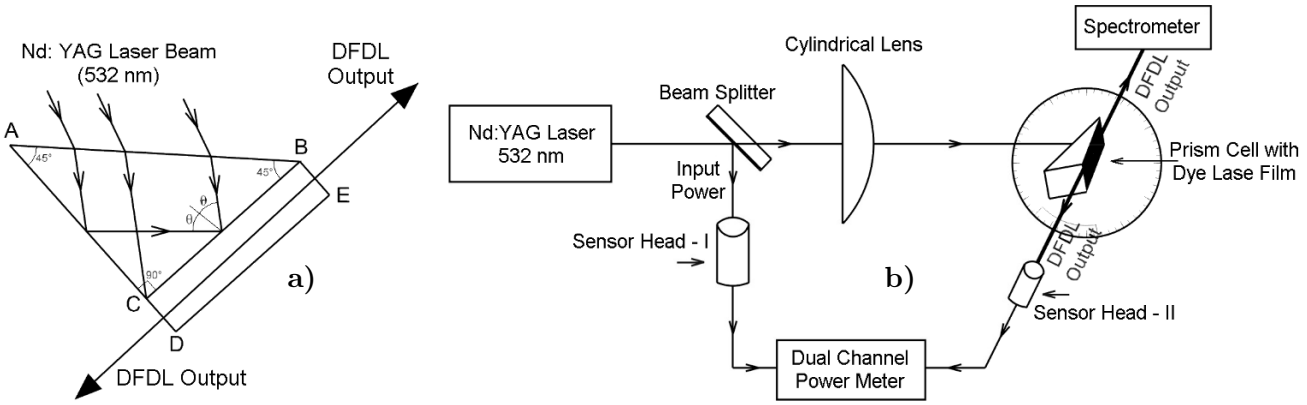

Fig. 5. Schematic diagram of the prism dye cell (a) and the experimental setup of DFDL (b).

prism and formed fringes on the dye cell, producing periodic modulation of the refractive index and also the gain. The DFDL output was obtained from side BC of the prism as shown in Fig. 5 b. These beams were made to interfere with the dye cell at different angles by rotating the dye cell set-up (donor–acceptor angles). Feedback was obtained via Bragg reflection due to a periodic structure incorporated throughout the active medium. For a pump beam of wavelength λ_{p} at angle θ on the medium, the DFDL wavelength is given by [27]

$$\lambda_{\mathrm{DFDL}} = \frac{n\lambda_{\mathrm{p}}}{n_p \sin\theta},$$

where n and n_p are the refractive indices of the dye solution and the prism material, respectively.

5. Results and Discussion

5.1. Thermal Stability of the Dye-Doped Polymer Film

Thermogravimetric analysis (TGA) and differential thermal analysis (DTA) were performed to identify the thermal stability of the dye-doped polymer film using a NETZSCH STA409C analyzer in nitrogen atmosphere at the heating rate of 10°C/min and temperature up to 800°C (Fig. 6). In the TGA curve, the weight losses occur at 386.8°C, which coincides with the DTA curve. This indicates that the material can retain its texture up to 386.8°C.

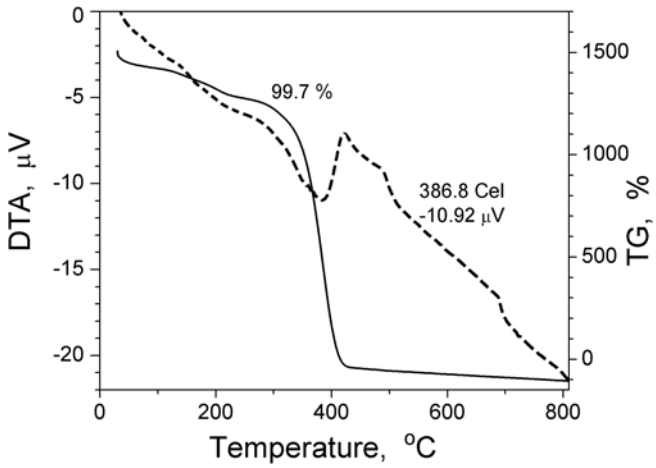

Fig. 6. TGA and DTA of the Pyronin-Y and cresyl violet dye doped with MMA.

5.2. DFDL Output Measurements

A *Q*-switched Nd:YAG laser was used as a pump source. To sense the input power being reflected from the beam splitter, a sensor (model J 10 LE YAG; sensor head-I) was connected to the power meter (EPM 2000; Coherent Molectron). Assuming the total DFDL output power to be equal on either side of the dye cell, we measure the DFDL

output energy from only one end, using a sensor (model J 50 MB YAG; sensor head II) connected to the power meter. Emission spectra were viewed using an OSM2 spectrometer. The DFDL output energies expressed as a function of the input pump power and donor–acceptor concentration were computed and are shown in Figs. 7 and 8. The experimental values (points) show good agreement with theoretical curves.

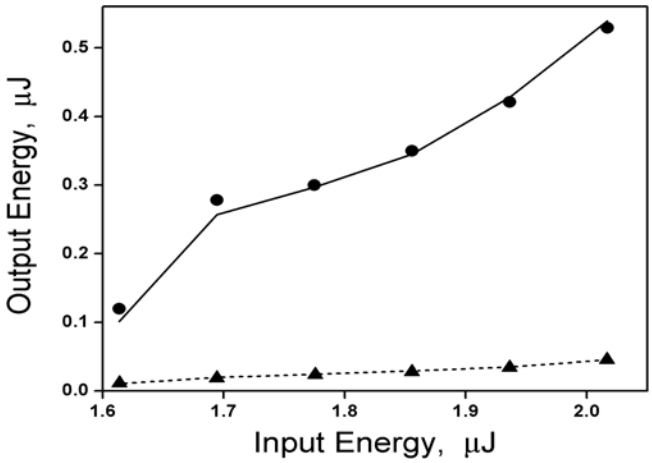

Fig. 7. Donor (●) and acceptor (▲) DFDL output energies as functions of the pump energy for fixed donor ($N_d = 1.8 \cdot 10^{18}$ cm^{-3}) and acceptor ($N_a = 0.6 \cdot 10^{18}$ cm^{-3}) concentrations. Here, theoretical results (dashed and solid curves) and experimental results (stars and filled circles).

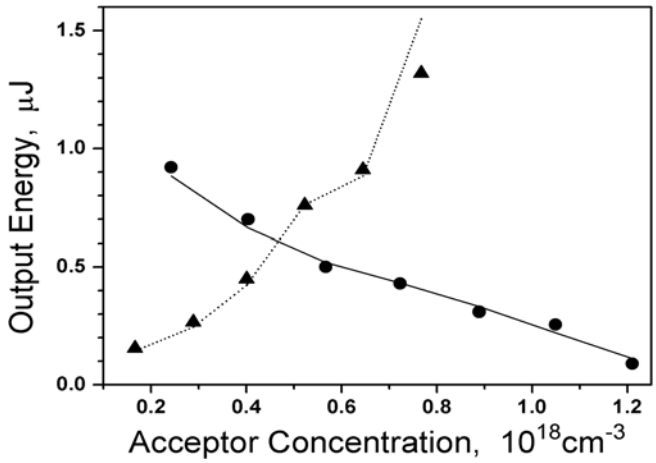

Fig. 8. Donor (●) and acceptor (▲) DFDL output energies as functions of the acceptor concentration for fixed pump power ($I_p = 0.8 \cdot 10^{22}$ cm^{-2}s^{-1}) and donor concentration ($N_d = 1.8 \cdot 10^{18}$ cm^{-3}), where the theoretical results are shown by the corresponding solid and dotted curves.

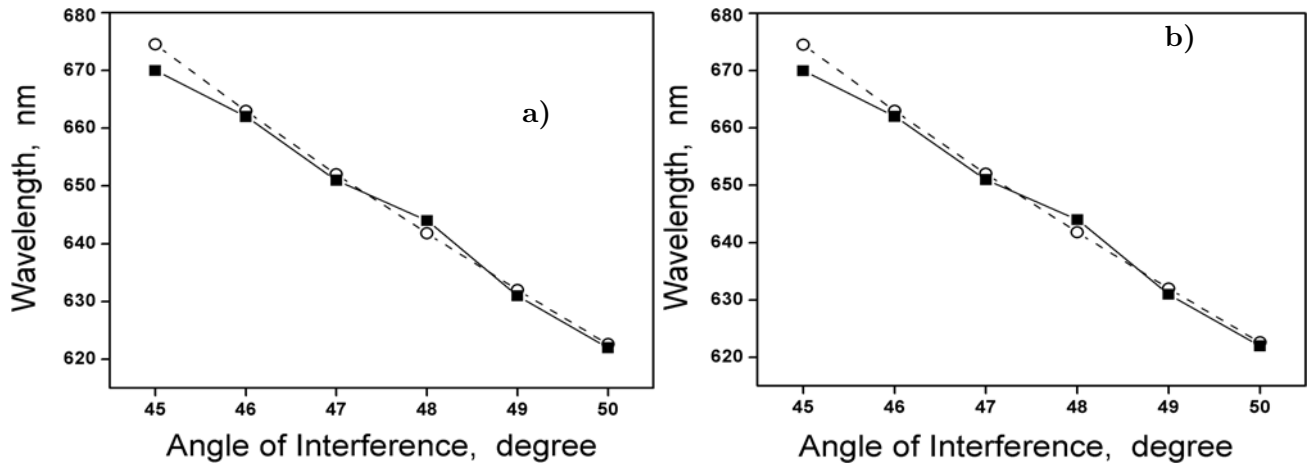

Fig. 9. Tunabilities of the donor (PY) DFDL (a) and the acceptor (CV) DFDL (b) as functions of the angle of interference θ. Here, theoretical results are shown by filled squares and experimental results, by circles.

5.3. Wavelength Tuning

We studied the wavelength-tunability potential of the title dyes singly and in combination. PY solution (3 mM) alone was taken and tunability of the DFDL was evaluated. By varying the angle of interference θ of the pump beam between 49° and 55°, we found the peak DFDL emission at 53°. When

the experiment was repeated with the dye mixture (3 mM PY and 1 mM CV) by varying the angle of interference between 45° and 50°, we found the peak DFDL emission at 50°. From spectrometric readings, the tunability range for PY (DFDL) only was between 580 and 622 nm, but for the dye mixture, the tunability extended up to 670 nm. Figure 9 shows the experimental and theoretical values of tunability of both DFDLs.

6. Conclusions

Organic PY and CV dyes were doped with MMA by the spin-coating method, and their energy transfer from the donor (PY) to the acceptor (CV) has been observed. We studied the effect of the donor and acceptor concentration and the pump power on the energy transfer and analyzed its mechanisms. The tunable range was found to be from 570 to 680 nm, which is greater than 90 nm.

References

1. B. H. Soffer and B. B. McFarland, *Appl. Phys. Lett.*, **10**, 266 (1967).
2. O. G. Peterson and B. B. Snavely, *Appl. Phys. Lett.*, **12**, 238 (1968).
3. M. Ahmad, T. A. King, D. K. Ko, et al., *Opt. Laser Tech.*, **34**, 445 (2002).
4. A. Costela, I. G. Moreno, C. Gomez, et al., *Chem. Phys. Lett.*, **387**, 496 (2004).
5. T. H. Nhung, M. Canva, T. T. A. Dao, et al., *Appl. Opt.*, **42**, 2213 (2003).
6. F. J. Duarte, *Appl. Opt.*, **33**, 3857 (1994).
7. D. A. Gromov, K. M. Dyumaev, A. A. Manenkov, et al., *J. Opt. Soc. Am. B*, **2**, 1028 (1985).
8. M. Berggern, A. Dodabalapur, R. E. Slusher, and Z. Bao, *Nature*, **389**, 466 (1997).
9. G. A. Kumar, V. Thomas, G. Jose, et al., *J. Photochem. Photobiol. A*, **153**, 145 (2002).
10. R. Sailaja and P. B. Bisht, *Org. Electron.*, **8**, 175 (2007).
11. T. Urisu and K. Kajiyama, *J. Appl. Phys.*, **47**, 3563 (1976).
12. D. Mohan, S. Sanghi, R. D. Singh, et al., *J. Photochem. Photobiol. A*, **68**, 77 (1992).
13. G. A. Kumar and N. V. Unnikrishnan, *J. Photochem. Photobiol. A*, **144**, 107 (2001).
14. M. Basheer Ahamed and P. K. Palanisamy, *Opt. Commun.*, **67**, 231 (2002).
15. N. Khan and T. A. Hall, *Opt. Commun.*, **228**, 177 (2003).
16. V. Dumarcher, L. Rocha, C. Denis, et al., *J. Opt. A: Pure Appl. Opt.*, **2**, 279 (2000).
17. H. Su and L. F. Luster, *J. Phys. D: Appl. Phys.*, **38**, 2112 (2005).
18. J. E. Bjorkholm and C. V. Shank, *Appl. Phys. Lett.*, **20**, 306 (1972).
19. H. Kogelink and C. V. Shank, *J. Appl. Phys.*, **43**, 2327 (1972).
20. M. I. Savadatti, S. R. Inamdar, N. N. Math, and A. D. Mulla, *J. Chem. Soc. Faraday Trans.*, **82**, 2417 (1986).
21. U. Tsuneno and K. Kajiyama, *J. Appl. Phys.*, **47**, 3563 (1976).
22. S. Speiser and R. Katraro, *Opt. Commun.*, **27**, 287 (1978).
23. O. G. Peterson and B. B. Snavely, *Bull. Am. Phys. Soc.*, **13**, 397 (1968).
24. W. Schmidt, W. Appt, and N. Wittekindt, *Z. Naturforsch. A.*, **27**, 37 (1972).
25. M. Basheer Ahamed, A. Ramalingam, and P. K. Palanisamy, *J. Lumin.*, **105**, 9 (2003).
26. M. Basheer Ahamed, R. G. Geethu Mani, and G. Vijayaraghavan, *Laser Phys.*, **22**, 1469 (2012).
27. S. Chandra, W. Takeuchi, and S. R. Hartmann, *Appl. Phys. Lett.*, **21**, 144 (1972).